Optical Properties of Gallium Oxide Clusters from First-Principles Calculations

ARTICLE *in* THE JOURNAL OF PHYSICAL CHEMISTRY A · OCTOBER 2012

Impact Factor: 2.69 · DOI: 10.1021/jp3084474 · Source: PubMed

3 AUTHORS:

Amol Rahane
K. T. H. M. College, Nashik, India
9 PUBLICATIONS **48** CITATIONS
SEE PROFILE

Mrinalini D. Deshpande
Gokhale Education Society´s H.P.T. Arts an…
20 PUBLICATIONS **243** CITATIONS
SEE PROFILE

Sudip Chakraborty
Uppsala University
31 PUBLICATIONS **48** CITATIONS
SEE PROFILE

THE JOURNAL OF PHYSICAL CHEMISTRY A

Article

pubs.acs.org/JPCA

Optical Properties of Gallium Oxide Clusters from First-Principles Calculations

Amol B. Rahane,[†,‡] Mrinalini D. Deshpande,*[,†] and Sudip Chakraborty[¶]

[†]Department of Physics, H.P.T. Arts and R.Y.K. Science College, Nasik, Maharashtra 422 005, India

[‡]Department of Physics, University of Pune, Pune, Maharashtra 411 007, India

[¶]Max-Planck-Institut für Eisenforschung GmbH, Max-Planck-Strasse 1, D-40237 Düsseldorf, Germany

ABSTRACT: The optical properties of the $(Ga_2O_3)_n$ clusters, with $n = 1-10$, have been studied within the framework of time dependent density functional theory. The gallium oxide cluster geometries showed evolution from planar configuration (C_{2v}) for Ga_2O_3 to layered globular configuration (C_s) for $(Ga_2O_3)_{10}$ via corundum configuration (D_{3d}) for $(Ga_2O_3)_4$. For $n \leq 5$, with the increase in coordination of Ga and O atoms, the polarizability decreases with the size of the cluster. For $n \geq 6$, with the stabilization of average coordination number for gallium and oxygen atoms, the decrease in polarizability is very small. Further, the optical absorption spectra and the corresponding optical gap have been calculated. The overall shape of the calculated spectra strongly depend on cluster geometries. With the increase in size, the discrete spectra of small clusters evolves into quasicontinuous spectra. For $n = 10$, the spectra show a smooth absorption edge that is a characteristic of the bulk. It is observed that the optical gap oscillate with an increase in the cluster size. The calculated optical gap of these clusters are lower than the band gap of α- and β-Ga_2O_3 phases. The underestimation of the calculated values of the cluster optical gap is due to the use of local density approximation.

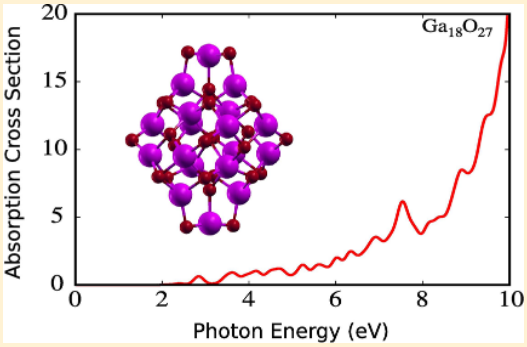

1. INTRODUCTION

The growth of optical communications has generated a great demand for efficient and low-cost materials to be used for light emission, detection and modulation. In addition to this, metal oxides have become important lasers and luminescent materials.[1,2] The catalytic properties of such oxides are recently envisaged as well. In the case of tight junction, its applicability as insulating barrier[3] has been recognized for the last couple of decades. The stable oxides of gallium can be used as dielectric coating of solar cell. Also, there is a huge demand of such oxides as transparent conductive materials.[4] A considerable amount of effort is carried out within different research communities to achieve these goals. Several materials and methods have emerged as possible contenders for optoelectronic industry. These include silicon based superlattices and quantum dots facilitating quantum confinement in silicon nanocrystals,[5−13] direct integration of III−V materials on semiconductor,[14,15] embedded carbon clusters in oxide or nitride matrices,[16] and IV−VI semiconductor nanocrystals,[12] superlattices with adsorbed oxygen.[17,18] All the mentioned techniques involve devices that are based on nanocrystalline materials.

In a nanostructure, potential barriers confine spatially electrons in the conduction band and holes in the valence band. Quantum confinement can act in three spatial directions, thus one has zero-dimensional (e.g., clusters, quantum dots), one-dimensional (e.g., nanowires), and two-dimensional (e.g., nanosheets, films) confined systems. Such quantum-confined structures have a number of commercial applications in lasers, optical amplifiers, and also in optical communications.[19,20] Fundamentally, quantum confinement pushes up the allowed energies effectively increasing the bandgap. This shift increases as the nanoparticle size becomes smaller. It also increases as the characteristic dimensionality of the quantum confinement increases (from 1D → 2D → 3D). Hence, quantum confinement may be used to tune the energy of the emitted light in nanoscale optical devices based on the nanoparticle size and shape. The other important fundamental issue is the momentum conservation in the optical transition. An exciton (analogous to hydrogen atom) is a pair of an electron and a hole bound to each other by Coulomb interaction with lesser binding energy than that of the hydrogen atom. In a nanoparticle the exciton binding energy increases due to the confinement induced overlap of the electron and hole wave functions.[10] Also the physical size and shape of the material strongly influences the nature and dynamics of the electronic excitation. Therefore, it is of interest to both physicists and chemists, because the excitons can be engineered in the material according to structure and also because the spatial confinement of the exciton accentuates many of its interesting physical properties.[21] There is a constantly growing interest in studying various properties of spatially confined atoms, molecules, and molecular complexes.

Received: August 25, 2012
Revised: October 8, 2012
Published: October 9, 2012

   dx.doi.org/10.1021/jp3084474 | J. Phys. Chem. A 2012, 116, 10559−10565

Recently, we have initiated a systematic study of the evolution of the structural and electronic properties of metal oxide clusters and reported the equilibrium structures, bonding nature, and electronic properties of $(Ga_2O_3)_n$ clusters[22] in the size range of $n = 1-10$. With this vivid and versatile background of quantum confinement effect and applications of metal oxide nanostructures, specifically we investigate the optical properties of $(Ga_2O_3)_n$ clusters. To do so, we have performed the calculations using the time dependent density functional theory (TDDFT) for $(Ga_2O_3)_n$ clusters and report here the results on the evolution of the optical properties of $(Ga_2O_3)_n$ clusters in the size range $n = 1-10$. We have also calculated the polarizabilities using finite-field method. The organization of the paper is as follows: section 2 deals with the computational method used in this work. The results are presented and discussed in section 3. Finally, we present our conclusions in section 4.

2. COMPUTATIONAL DETAILS

The lowest energy and low-lying configurations for $(Ga_2O_3)_n$ clusters in the size range $n = 1-10$ have been adopted from our previous study.[22] The calculations were performed by using the Vienna ab Initio Simulation Package (VASP) code.[23,24] The generalized gradient approximation (GGA) given by Perdew–Bruke–Ernzerhof[25] and the projector augmented wave (PAW) method[26,27] were used.

The polarizabilities and optical spectra for the lowest energy and some of the low-lying configurations are calculated using a real space formalism within time dependent local density approximation (TDLDA).[28,29] The TDLDA formalism is a very popular approach for the calculations of excitation energies and optical spectra. This technique has recently been applied to several clusters and was found to yield results in very good agreement with experiments.[29−38] For this, initially a static calculations of the wave function optimization is performed for the optimized geometry of the clusters within the DFT formalism, using PARSEC code.[39,40] We have used norm-conserving Troullier–Martins pseudopotentials,[41] and the exchange–correlation energy has been calculated using the Ceperley–Alder data[42] with Perdew–Zunger parametrization.[43] PARSEC offers an effective way for computing optical excitation spectra, based on a formalism that circumvents explicit propagation of wave functions in time. This is achieved by determining optical transition energies and oscillator strengths from the poles and residues, respectively, of the dynamic polarizability.[44] In this approach, the Kohn–Sham eigenvalues and eigenfunctions are used to construct a new eigenvalue problem, in the form:

$$[\omega_{ij\sigma}{}^2\delta_{ik}\delta_{jl}\delta_{\sigma\tau} + 2\sqrt{f_{ij\sigma}\,\omega_{ij\sigma}}\,K_{ij\sigma,k l\tau}\sqrt{f_{kl\tau}\,\omega_{kl\tau}}\,]F_n = \Omega^2 F_n \quad (1)$$

where Ω_n are the optical excitation energies, $\omega_{ij\sigma} = \varepsilon_{j\sigma} - \varepsilon_{i\sigma}$ are the Kohn–Sham transition energies, and $f_{ij\sigma} = n_{i\sigma} - n_{j\sigma}$ are the differences between the occupation numbers of the ith and jth states. The eigenvectors F_n are related to the oscillator strength, and $K_{ij\sigma kl\tau}$, is a coupling matrix given by

$$K = \iint \phi_{i\sigma}(r)\,\phi_{j\sigma}(r)\left(\frac{1}{|r - r'|} + \frac{\delta^2 E_{xc}[\varrho]}{\delta\varrho_\sigma(r)\,\delta\varrho_\tau(r')}\right)\phi_{k\tau}(r')\,\phi_{l\tau}(r')\,dr\,dr' \quad (2)$$

where $\phi(r)$ are the one-electron Kohn–Sham orbitals, and the indices i, j, σ (as well as k, l, τ) indicate for occupied states, unoccupied states, and spin, respectively.

The converged Kohn–Sham eigenvalues and eigenfunctions are obtained from the PARSEC code and then using RGWBS code[29] (a compatible "TDDFT" package), the coupling matrix is first evaluated in real-space and then used to solve eq 1, from the solutions of which an optical excitation spectrum can be constructed easily.

The strength of the absorption associated with the transition energy Ω_n, denoted by f_n, is related to the eigenvector F_n by[45]

$$f_n = \frac{2}{3}\sum_{\beta=1}^{3} |B_\beta^T R^{1/2} F_n|^2 \quad (3)$$

where

$$R_{ij,kl} = \delta_{ik}\delta_{jl}\lambda_{kl}\omega_{kl} \quad \text{and} \quad (B_\beta)_{ij} = \int \phi_i^*(r) r_\beta \phi_j(r)\,dr \quad (4)$$

and $\{r_1, r_2, r_3\} = \{x, y, z\}$. Ω_n and f_n define the absorption spectrum uniquely and the TDDFT computation is complete.

In the real space formalism, we have used the grid spacing $h = 0.4$ a.u. The grid was set up inside a spherical boundary with a radius of 18 au polarizabilities were calculated using a finite-field approach[46,47] with a grid spacing of $h = 0.4$ a.u., radius of the spherical boundary of 18 au, and an applied external electric field of 10^{-3} Ry/au. The spectra are calculated slightly on a larger grid and spherical boundary radius. Inclusion of about triple that of occupied states was found to be sufficient to obtained well converged spectra. We carefully tested convergence of the calculated excitation energies and absorption spectra with respect to the size of the spherical boundary domain, the grid spacing, and the total number of electronic states included in calculations.

3. RESULTS AND DISCUSSION

Earlier, we have explored the structural and electronic properties of $(Ga_2O_3)_n$ clusters, with $n = 1-10$, using density functional theory.[22] Overall, for gallium oxide clusters with bulk stoichiometry $(Ga_2O_3)_n$, with the increase in n, we found the strong competition between two structural motifs: the rhombus (Ga_2O_2) and the planar or chairlike hexagonal (Ga_3O_3) units. With these two building blocks, the hollow globular configurations that were evolved with a large number of rhombus units may be related with a progression toward the bulk-like behavior. There are 3-, 4-, and 5-fold coordinated Ga atoms and 2-, 3-, and 4-fold coordinated oxygen atoms. The $(Ga_2O_3)_n$ structures have similarity to that of the α-Ga_2O_3 phase, and the average coordination of Ga- and O-atoms in clusters are lower than the values in the α-Ga_2O_3. It is seen that the stability of different isomers of a cluster with a given size depends upon the number of four- and six-membered rings and their distribution. Such four- and six-membered rings are also found in nanoparticles of Al_2O_3,[48] In_2O_3,[49] GaN,[50] and other compounds in which the metal–oxygen interactions are strongly ionic. With the increase in cluster size, the charge transfer from Ga atoms to oxygen increases toward the value in bulk. The stability of the cluster is dominated by ionic Ga–O interactions with some covalent character between Ga-sp and O-p orbitals. A sequential addition of a Ga_2O_3 unit to the $(Ga_2O_3)_n$ cluster initially increases the binding energy, though values of the highest occupied molecular orbital-lowest

dx.doi.org/10.1021/jp3084474 | J. Phys. Chem. A 2012, 116, 10559−10565

unoccupied molecular orbital gap (HOMO−LUMO), do not show any systematic variation in these clusters. All the lowest energy configuration of these clusters in this size range, prefer the lowest spin state.

Before discussing the results for the polarizabilities and the optical spectra of these clusters, we would like to note that we have also performed the optimization of some of the lowest and low-lying configurations of gallium oxide clusters using LDA. We did not observe any significant differences between the LDA(CA) and GGA(PBE) optimized geometries for the selected clusters. The switch from GGA to LDA does not seem to affect the overall shapes, GGA calculations predict larger bond lengths than LDA bond lengths; e.g., for the $(Ga_2O_3)_{10}$ cluster, the Ga−O bond lengths using GGA varies between 1.78 and 2.08 Å. The use of LDA slightly shortens the bond lengths, which varies between 1.75 and 2.07 Å. This result agrees with a common observation that GGA corrects the overbinding tendency of LDA.[51]

The calculated polarizabilities per atom for $(Ga_2O_3)_n$ clusters for $n = 1-10$ are shown in Figure 1. In all cases, polarizabilities

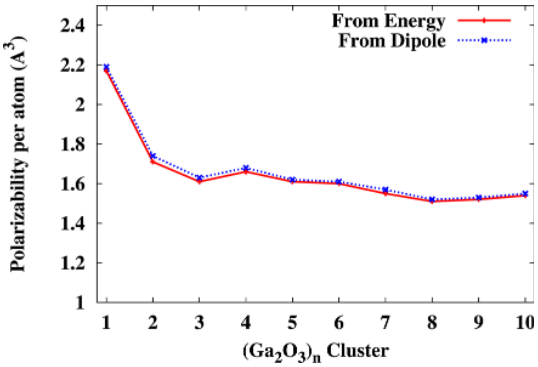

Figure 1. Polarizabilities per atom for $(Ga_2O_3)_n$ clusters vs the size of the cluster (n).

calculated from the total energy and from the dipole moment coincided within 1%.[52] It is seen that, with the successive addition of Ga_2O_3 unit, the coordination number of Ga and O atoms increases, the stability of the cluster increases which results in decrease in the polarizability of the cluster. For Ga_2O_3, the polarizability is 2.2 Å. For $n = 5$, it decreases up to 1.6 Å. For $n \leq 5$, with the increase in coordination of Ga and O atoms, the polarizability decreases with size of the cluster. From $n = 6$, overall the structures are stabilized with the coordination of four for Ga atoms and three for O atoms. For the clusters with $n \geq 6$, the polarizability per atom decreases slowly with the increase in cluster size. The observed trend of decrease in the polarizability with the cluster size is consistent with that of reported studies on metal clusters.[53] Further, we have also compared the average Ga−O bond lengths with that of the polarizability of the cluster. It is observed that with the decrease in the average Ga−O bond length the polarizability decreases. From the analysis of the charge density plots (not shown), it is observed that as the coordination of Ga atom increases, the high charge density around Ga cation distorts the electron cloud around the ion in contact with it, causing the polarization. In the lowest energy configuration the delocalize Ga-4s and Ga-4p significantly alter charge density around oxygen (delocalization of O-p states) which result in decrease in polarizability.

In Figure 2, we present TDLDA absorption spectra of the $(Ga_2O_3)_n$ clusters, with $n = 1-10$. As the size of the cluster

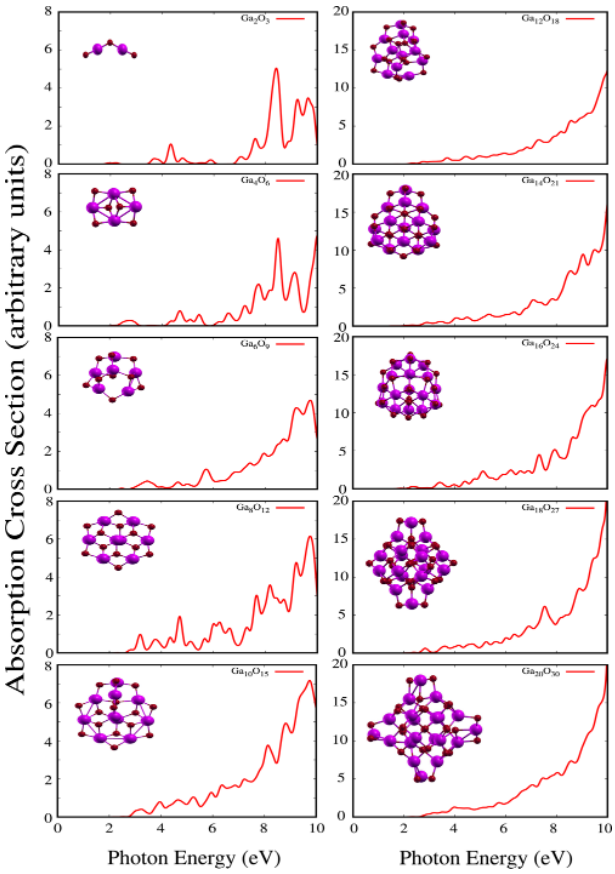

Figure 2. TDLDA optical absorption spectra of the $(Ga_2O_3)_n$ clusters for $n = 1-10$. A Gaussian convolution of 0.1 eV has been used to simulate a finite broadening of the calculated spectra.

increases, the discrete spectra of small clusters evolves into quasicontinuous spectra. It can be seen that for $n \leq 5$, the spectra of $(Ga_2O_3)_n$ clusters are dominated by discrete, atomic-like transitions. Unlike optical spectra of semiconductor clusters with open surfaces,[38] the TDLDA spectra of gallium oxide clusters display the low energy transitions associated with the surface states. With the increase in coordination number of Ga and O atoms, it is seen that the oscillator strength in absorption spectra is spread over a wide energy range, thus leading to broader overall spectra.

To understand the evolution of optical spectra in further detail, we have analyzed the site projected density of states (PDOS) for Ga and O atoms. In Figure 3, we have shown the PDOS for some of the cases like, $n = 1, 4, 8$, and 10. It is seen that, for small sized clusters, the electronic spectra for Ga and O atoms show sharp peaks but with the increase in cluster size, the spectra become broader. The calculated PDOS on Ga and O atoms further show that the energy levels near HOMO consists of the contribution from O-2p states, whereas the states near the LUMO consist of the contribution from Ga-4s as well as O-2p states. The middle part of the spectra consists of hybridized Ga-sp and O-p states along with the nonbonding O-p states from the 3-fold coordinated oxygen atoms. It is observed that with the increase in n, the coordination number

dx.doi.org/10.1021/jp3084474 | J. Phys. Chem. A 2012, 116, 10559−10565

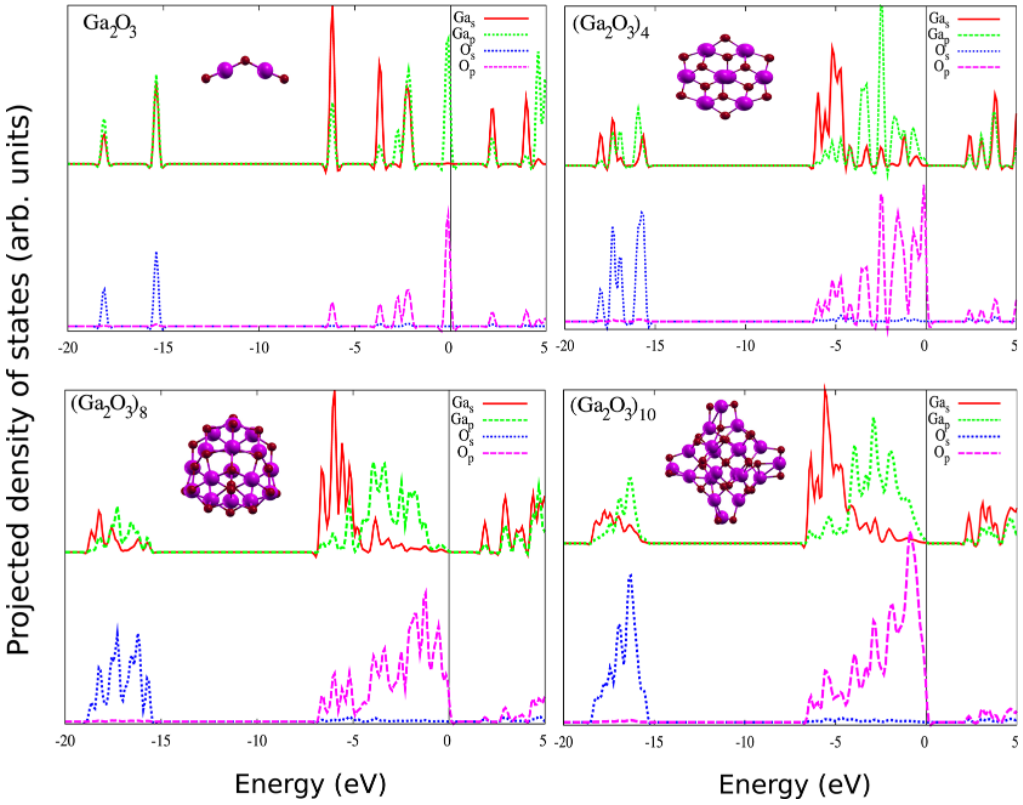

Figure 3. Site projected density of states (PDOS) for the lowest energy configurations for $(Ga_2O_3)_n$ clusters, with $n = 1, 4, 8$, and 10. The Fermi level, given by the dotted line, is aligned to zero.

of Ga and O atoms increases which results in more charge transfer from Ga to O atom. In small sized clusters ($n \leq 4$), there seems to be more contribution from covalent bonding between Ga and O atoms, and that could also be the reason for a localized spectrum. One can easily conclude that the first few peaks in the absorption spectrum arising from the transition between O-2p and Ga-4s states. The higher energy peaks in the absorption spectra are due to 2p states of the oxygen atoms. It is seen that with the increase in the coordination of O atoms, the 2p spectra of the 3-fold coordinated oxygen became broader which results in the broadening of the corresponding transitions region in the optical spectra.

It can be seen that the spectra of small clusters are dominated by discrete, atomic-like transitions. For the Ga_2O_3 cluster, the first dominant peak is approximately nearer to 8 eV, which occurs due to transition between HOMO−1 and LUMO+3 state. The other dominant peaks correspond to transitions between the HOMO−1 to LUMO and HOMO to LUMO. The development of one additional peak is closely related to the involvement of the O-p orbitals. For $n = 2$, the change in the spectra is attributed to the transition from the two-dimensional (2D) to three-dimensional (3D) geometries. Addition of Ga_2O_3 unit distort the $(Ga_2O_3)_2$ structure more significantly. With the increase in Ga and O coordination, the distortion in the cluster geometry further reduces the energy of the newly populated level in $(Ga_2O_3)_3$. It reduces the oscillator strengths and the splitting of the absorption peaks. The structural variation causes significant changes in the absorption spectrum of $(Ga_2O_3)_3$ as compared to that of $(Ga_2O_3)_2$. Addition of one more (Ga_2O_3) unit to $(Ga_2O_3)_3$ makes the structure more symmetric. The lowest energy configuration appears to be derived from the bulk corundum (α-Ga_2O_3) configuration. As compared to $(Ga_2O_3)_3$, the number of high intensity peaks increases with the broadening of the spectra, which reflect in an increase in hybridization of the Ga-s and O-p bands. From $n = 6-10$, the structures are stabilized with the coordination of four for Ga atoms and three for O atoms. For clusters with $n \geq 6$, the transition from discrete, atomic-like excitations to quasicontinuous spectra is observed. For $n = 10$, the spectra shows a smooth absorption edge which is a characteristic of the bulk.[54,55]

Table 1 shows the transitions from the occupied state to empty state that contribute to the first peak in the absorption spectra of $(Ga_2O_3)_n$ clusters, with $n = 1-10$. From the analysis of the excitations, the dominant contribution to the first peak is from transition between HOMO to LUMO level. It is observed that for the Ga_2O_3 cluster the HOMO level is triply degenerate state. It is observed that, for the Ga_2O_3 cluster the first peak near 2 eV and a peak near 3.66 eV has a dominant contribution from the triply degenerate HOMO to LUMO level transition. For Ga_4O_6 the first peak near 2.70 eV corresponds to the transition between HOMO and LUMO level. The transition from HOMO−1 to LUMO level is seen in the peak near 2.95 eV. For Ga_8O_{12} cluster, the first peak near 2.85 eV is due to the transition from HOMO to LUMO level, whereas the transition from HOMO−1 to the LUMO level has energy near 2.95 eV. For $Ga_{20}O_{30}$ cluster, the first transition near 2.96 eV is due to the transition from HOMO to LUMO levels, whereas the peak at 3.22 eV is due to the transition from HOMO to LUMO+1 level. Overall, it is seen that the first TDLDA transitions are

dx.doi.org/10.1021/jp3084474 | J. Phys. Chem. A 2012, 116, 10559−10565

Table 1. Transitions (Denoted as Occupied State → Empty State) that Contribute to the First Peak in the Absorption Spectra of $(Ga_2O_3)_n$ Clusters ($n = 1-10$)[a]

cluster	energy (eV)	transition	%
Ga_2O_3	2.01	HOMO → LUMO	99.70
		other	0.30
Ga_4O_6	2.70	HOMO → LUMO	96.41
		other	3.59
Ga_6O_9	3.32	HOMO → LUMO	95.61
		HOMO−1 → LUMO	2.41
		other	1.58
Ga_8O_{12}	2.85	HOMO → LUMO	94.50
		other	5.50
$Ga_{10}O_{15}$	3.08	HOMO → LUMO	99.19
		other	0.81
$Ga_{12}O_{18}$	3.05	HOMO → LUMO	97.16
		other	2.84
$Ga_{14}O_{21}$	2.02	HOMO → LUMO	99.82
		other	0.18
$Ga_{16}O_{24}$	2.91	HOMO → LUMO	96.81
		other	3.19
$Ga_{18}O_{27}$	2.70	HOMO → LUMO	96.95
		other	3.05
$Ga_{20}O_{30}$	2.96	HOMO → LUMO	99.15
		other	0.85

[a]The % column shows the percentage contribution of a particular transition.

dominated by a single-level to single-level transition. For all the clusters, the first peak appears due to transition between HOMO and LUMO level.

For the calculation of the optical gap we have used the strategy implemented by previous studies.[32,33] The first optical absorption gap is defined as the energy of the first allowed dipole transition. But usually this criterion is impractical because the intensity of the first allowed transition could be extremely weak depending upon the oscillator strength. Hence, an effective optical gap, $\Omega_g(p)$ is calculated using a certain cutoff value defined as

$$\int_0^{\Omega_g(p)} \sigma(\omega)\, d\omega = pf_e \qquad (5)$$

where $\sigma(\omega)$ is the photoabsorption cross-section per electron, f_e is the complete one electron oscillator strength defined as $f_e = 2\pi^2\hbar e^2/mc \sim 1.098$ eV Å^2, and p is small positive number whose value is taken as 0.02.

Table 2 represents the first optical gap using TDDFT (LDA-CA) along with the average coordination numbers of Ga and O atoms for the $(Ga_2O_3)_n$ clusters with $n = 1-10$. With the increase in cluster size, the optical gap continues to exhibit an oscillatory behavior. It is observed that the variation of the first optical gap is consistent with the average coordination number of O atoms. As the coordination number of oxygen atoms increases, the optical gap decreases. Note that the experimental band gap[56] for the bulk α-Ga_2O_3 is 4.98 eV, and β-Ga_2O_3 is 4.8 eV. It is known that the use of GGA and LDA underestimates the HOMO−LUMO gap; hence the values of optical gaps are also underestimated due to the use of LDA.

It is seen that the optical spectra and optical gap are dependent on the shape and size of the cluster and hence it can be varied by solely managing the shape of the nanostructures. To understand the variation in the optical spectra according to

Table 2. First Optical Absorption Gap Using TDDFT (LDA-CA) and Average Coordination Numbers of Ga Atom and O Atom for $(Ga_2O_3)_n$ Clusters, with $n = 1-10$

		average coordination	
cluster	optical gap (eV)	Ga atom	O atom
Ga_2O_3	3.51	2.00	1.33
Ga_4O_6	2.47	3.50	2.33
Ga_6O_9	2.98	3.33	2.22
Ga_8O_{12}	2.82	3.75	2.50
$Ga_{10}O_{15}$	2.95	3.70	2.46
$Ga_{12}O_{18}$	2.47	3.75	2.50
$Ga_{14}O_{21}$	2.22	4.14	2.76
$Ga_{16}O_{24}$	2.26	4.25	2.83
$Ga_{18}O_{27}$	2.46	4.16	2.77
$Ga_{20}O_{30}$	2.51	4.15	2.76

the symmetry of the cluster, we have considered some of the isomers of $(Ga_2O_3)_{10}$ cluster. In Figure 4, we have presented the optical absorption spectra along with the optical gap for some of the globular configurations[22] for the $(Ga_2O_3)_{10}$ cluster. The average coordination numbers of oxygen atoms in these configurations are 2.26 (D_2), 2.33 (D_{5d}), 2.0 (D_{3h}), and 2.0 (I_h), respectively. The calculated first optical gaps are 2.67 eV for D_2, 2.56 eV for D_{5d}, 3.01 eV for D_{3h}, and 2.92 eV for I_h configuration. The optical gap varies with the variation in cluster symmetry. It is noted that the optical gap decreases with the increase in average coordination of oxygen atoms. With the decrease in Ga and O atoms coordination, there is an increase in the nonbonding 2p states near HOMO. This results into the variation in the overall optical spectra as well as optical gap of the configuration.

The experimental optical emission spectra of the Ga_2O_3 nanostructures was studied by Zhou et al.[57] They observed four types of transition peaks in the spectrum, namely UV (3.41 eV), red (1.78 eV), blue (2.75 eV), and yellow (2.35 eV) emission. The UV and red emissions from the Ga_2O_3 nanostructures are from the amorphous shell of the nanostructures, whereas the blue and yellow emissions are from the crystalline β-Ga_2O_3 core. If we compare the absorption spectrum of gallium oxide clusters, for $n = 1$, 2, and 3, the first peaks (as shown in Table 1) in the spectrum for small clusters are 2.01, 2.70, and 3.32 eV, respectively. For the large size clusters, the first peak for most of the clusters falls in the region 2.70−3.08 eV except $n = 7$. The comparison shows that the blue transitions in the larger clusters may be the outcome of the bulklike coordination for these clusters. We hope that these clusters considered here would offer valuable assistance to future experimental and theoretical studies on gallium oxide nanostructures. The present study should also provide some important information to facilitate the designs and applications of nanoscaled-gallium oxide based materials, in the field of optoelectronic devices.

4. CONCLUSIONS

We have studied the structural and optical properties of $(Ga_2O_3)_n$ clusters, with $n = 1-10$. For gallium oxide clusters with bulk stoichiometry $(Ga_2O_3)_n$, with the increase in size (n), we found the strong competition between two structural motifs: the rhombus (Ga_2O_2) and the planar or chairlike hexagonal (Ga_3O_3) units. With these two building blocks, the hollow globular configurations that were evolved with a large number of rhombus units may be related with a progression

dx.doi.org/10.1021/jp3084474 | J. Phys. Chem. A 2012, 116, 10559−10565

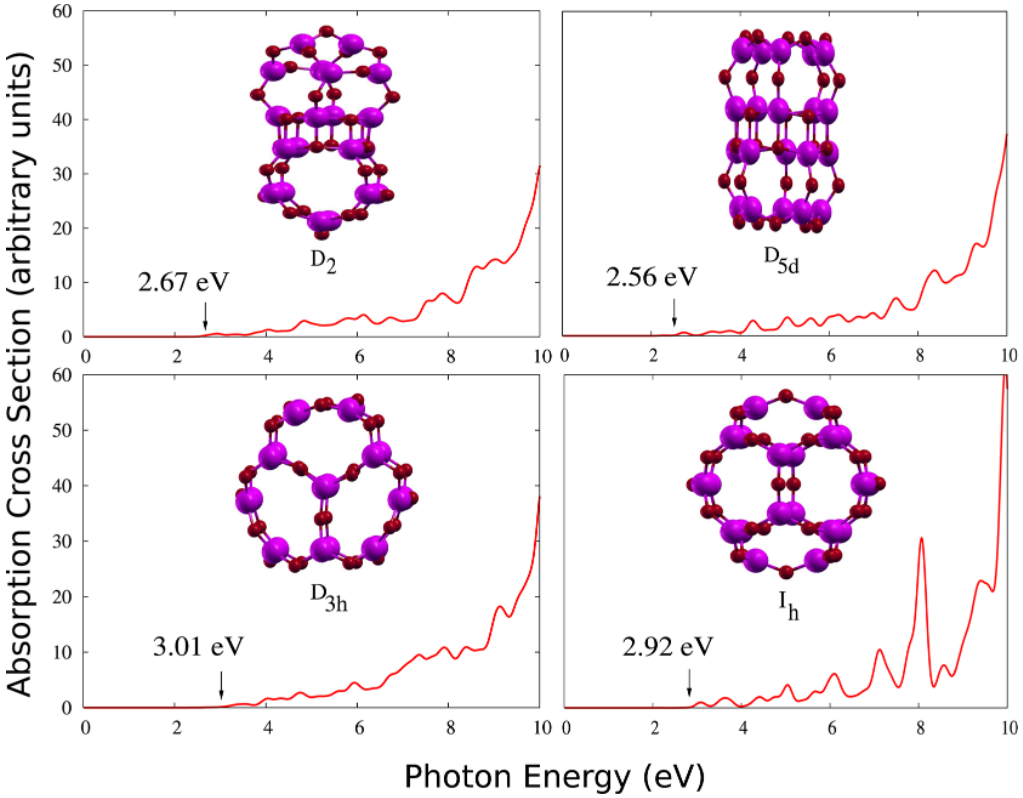

Figure 4. Shape dependent optical absorption spectra for cage type configurations of $(Ga_2O_3)_{10}$ cluster. The values in electronvolts represent the optical gap for the specific configuration.

toward the bulk-like behavior. For $n \leq 5$, with the increase in coordination of Ga and O atoms, the polarizability decreases with size of the cluster. From $n = 6$, overall the structures are stabilized with the coordination of four for Ga atoms and three for O atoms. For the clusters with $n \geq 6$, the polarizability per atom decreases slowly with the increase in cluster size. It is seen that the optical spectra and optical gaps are dependent on the shape and size of the cluster. As the size of the cluster increases, the discrete spectra of small clusters evolves into quasicontinuous spectra. It can be seen that for $n \leq 5$, the spectra of $(Ga_2O_3)_n$ clusters are dominated by discrete, atomic-like transitions. For $n = 10$, the spectra shows a smooth absorption edge, which is a characteristic of the bulk. With the increase in cluster size, the optical gap continues to exhibit an oscillatory behavior. With the increase in cluster size the dominant peaks shifted toward the higher energy range. This shift is usually called as blue shift which is common in optical properties of nanoclusters. It is seen that the TDLDA transition is dominated by a single-level to single-level transition.

AUTHOR INFORMATION

Corresponding Author
*E-mail: d_mrinal@yahoo.com.

Notes
The authors declare no competing financial interest.

ACKNOWLEDGMENTS

M.D.D. and A.B.R. acknowledges financial assistance from the Department of Science and Technology (DST), Government of India, University Grants Commission (UGC), and Council for Scientific and Industrial Research (CSIR), New Delhi. We also acknowledge the Department of Physics, University of Pune, and the Center for Development of Advance Computing (CDAC), Pune and Bangalore, for providing the supercomputing facilities. We gratefully acknowledge Prof. D. G. Kanhere for helpful discussions. The Max-Planck Society is also kindly acknowledged by S.C.

REFERENCES

(1) Shimizu, K.; Takamatsu, M.; Nishi, K.; Yoshida, H.; Satsuma, A.; Tanaka, T.; Yoshida, S.; Hattori, T. J. Phys. Chem. B 1999, 103, 1542.
(2) Bailar, J.; Emeleus, H.; Nyholm, R.; Trotman-Dickenson, A. Comprehensive Inorganic Chemistry 1973, 1, 1091.
(3) Dai, Z. R.; Pan, Z. W.; Wang, Z. L. J. Phys. Chem. B 2002, 106, 902.
(4) Rebien, M.; Henrion, W.; Hong, M.; Mannaerts, J. P.; Fleischer, M. Appl. Phys. Lett. 2002, 81, 250.
(5) Sung, G. Y.; Park, N. M.; Shin, J. H.; Kim, K. H.; Kim, T. Y.; Cho, K. S.; Huh, C. IEEE J. Sel. Top. Quant. Electron. 2006, 12, 1545.
(6) Tsu, R.; Zhang, Q.; Filios, A. Proc. SPIE 1998, 3290, 246.
(7) Luppi, E.; Degoli, E.; Cantele, G.; Ossicini, S.; Magri, R.; Ninno, D.; Bisi, O.; Pulci, O.; Onida, G.; Gatti, M.; Incze, A.; Del Sole, R. Opt. Mater. 2005, 27, 1008.
(8) Luppi, M.; Ossicini, S. Phys. Rev. B 2005, 71, 035340.
(9) Kholod, A. N.; Ossicini, S.; Borisenko, V. E.; Arnaud d'Avitaya, F. Surf. Sci. 2003, 30, 527.
(10) Filios, A. A.; Ryu, Y. S.; Shahrabi, K. Tech. Interface J./Winter Special Issue 2009, 10(2).
(11) Degoli, E.; Ossicini, S. Adv. Quantum Chem. 2009, 58, 203.
(12) Leitsmann, R.; Bechstedt, F. ACS Nano 2009, 3, 3505.
(13) Amato, M.; Palummo, M.; Ossicini, S. Phys. Status Solidi B 2010, 247, 2096.

(14) Iori, F.; Degoli, E.; Palummo, M.; Ossicini, S. *Superlattices Microstruct.* 2008, *44*, 337.
(15) Fang, A. W.; Park, H.; Jones, R.; Cohen, O.; Paniccia, M. J.; Bowers, J. E. *IEEE Photonics Technol. Lett.* 2006, *18*, 1143.
(16) Tsu, R.; Filios, A.; Zhang, Q. *Adv. Sci. Technol.* 1997, *27*, 55.
(17) Tsu, R.; Filios, A.; Lofgren, C.; Dovidenko, K.; Wang, C. G. *Electrochem. Solid State Lett.* 1998, *1*, 80.
(18) Zhang, Q.; Filios, A.; Lofgren, C; Tsu, R. *Physica E* 2000, *8*, 365.
(19) Castrejon, R. G.; Filios, A. *J. Lightwave Technol.* 2006, *24*, 4912.
(20) Filios, A.; Castrejon, R. G.; Tomkos, I.; Hallock, B.; Vodhanel, R.; Coombe, A.; Yuen, W.; Moreland, R.; Garrett, B.; Duvall, C.; Hasnain, C. C. *IEEE Photonics Technol. Lett.* 2003, *15*, 599.
(21) Scholes, G. D.; Rumbles, G. *Nat. Mater.* 2005, *5*, 683.
(22) Rahane, A. B.; Deshpande, M. D. *J. Phys. Chem. C* 2012, *116*, 2691.
(23) Kresse, G.; Furthmuller, J. *Phys. Rev. B* 1996, *54*, 11169.
(24) *Vienna ab initio Simulation Package (VASP)*, Technische Universität Wien, 1999.
(25) Perdew, J. P.; Burke, K.; Ernzerhof, M. *Phys. Rev. Lett.* 1996, *77*, 3865.
(26) Blöchl, P. E. *Phys. Rev. B* 1994, *50*, 17953.
(27) Kresse, G.; Joubert, D. *Phys. Rev. B* 1999, *59*, 1758.
(28) Kronik, L.; Makmal, A.; Tiago, M. L.; Alemany, M. M. G.; Jain, M.; Huang, X.; Saad, Y.; Chelikowsky, J. R. *Phys. Status Solidi B* 2006, *243*, 1063.
(29) Tiago, M. L.; Chelikowsky, J. R. *Phys. Rev. B* 2006, *73*, 205334.
(30) Bai, Y.-L.; Chen, X.-R.; Yang, X.-D.; Zhou, X.-L. *J. Phys. B* 2003, *36*, 4511.
(31) Yabana, K.; Bertsch, G. F. *Phys. Rev. A* 1999, *60*, 3809.
(32) Vasiliev, I.; Ogut, S.; Chelikowsky, J. R. *Phys. Rev. B* 2002, *65*, 115416.
(33) Nanavati, S. P.; Sundararajan, V.; Mahamuni, S.; Kumar, V.; Ghaisas, S. V. *Phys. Rev. B* 2009, *80*, 245417.
(34) Idrobo, J. C.; Ogut, S.; Jellinek, J. *Phys. Rev. B* 2005, *72*, 085445.
(35) Baishya, K.; Idrobo, J. C.; Ogut, S.; Yang, M. L.; Jackson, K.; Jellinek, J. *Phys. Rev. B* 2008, *78*, 075439.
(36) Harb, M.; Rabilloud, F.; Simon, D.; Rydlo, A.; Lecoultre, S.; Conus, S.; Rodrigues, V.; Felix, C. *J. Chem. Phys.* 2008, *129*, 194108.
(37) Tiago, M. L.; Idrobo, J. C.; Ogut, S.; Jellinek, J.; Chelikowsky, J. R. *Phys. Rev. B* 2009, *79*, 155419.
(38) Vasiliev, I.; Ogut, S.; Chelikowsky, J. R. *Phys. Rev. B* 1999, *60*, R8477.
(39) Alemany, M. M. G.; Jain, M.; Kronik, L.; Chelikowsky, J. R. *Phys. Rev. B* 2004, *69*, 075101.
(40) Chelikowsky, J. R.; Troullier, N.; Saad, Y. *Phys. Rev. Lett.* 1994, *72*, 1240.
(41) Troullier, N.; Martins, J. L. *Phys. Rev. B* 1991, *43*, 1993.
(42) Ceperley, D. M.; Alder, B. J. *Phys. Rev. Lett.* 1980, *45*, 566.
(43) Perdew, J. P.; Zunger, A. *Phys. Rev. B* 1981, *23*, 5048.
(44) Casida, M. E. In *Recent Advances in Desity Functional Methods, Part 1*; Casida, D. P., Ed.; World Scientific: Singapore, 1995; p 155. Casida, M. E. In *Recent Developments and Applications of Modern Density Functional Theory*; Seminario, J. K., Ed.; Elsevier: Amsterdam, 1996; p 391.
(45) Burdick, W. R.; Saad, Y.; Kronik, L.; Vasiliev, I.; Jain, M.; Chelikowsky, J. R. *Comput. Phys. Commun.* 2003, *156*, 22.
(46) Kurtz, H. A.; Stewart, J. J. P.; Dieter, K. M. *J. Comput. Chem.* 1990, *11*, 82.
(47) Quong, A. A.; Pederson, M. R. *Phys. Rev. B* 1992, *46*, 12906; *ibid.* 1992, *46*, 13584.
(48) Rahane, A. B.; Deshpande, M. D.; Kumar, V. *J. Phys. Chem. C* 2011, *115*, 18111.
(49) Walsh, A.; Woodley, S. M. *Phys. Chem. Chem. Phys.* 2010, *12*, 8446.
(50) Kandalam, A. K.; Blanco, M. A.; Pandey, R. *J. Phys. Chem. B* 2002, *106*, 1945.
(51) Zope, R. R.; Blundell, S. A.; Baruah, T.; Kanhere, D. G. *J. Chem. Phys.* 2001, *115*, 2109.
(52) Deshpande, M. D.; Kanhere, D. G.; Vasiliev, I.; Martin, R. M. *Phys. Rev. B* 2003, *68*, 035428.
(53) Alipour, M.; Mohajeri, A. *J. Phys. Chem. A* 2010, *114*, 12709.
(54) He, H.; Orlando, R.; Blanco, M. A.; Pandey, R.; Amzallag, E.; Baraille, I.; Rerat, M. *Phys. Rev. B* 2006, *74*, 195123.
(55) Lovejoy, T. C.; Chen, R.; Yitamben, E. N.; Shutthanadan, V.; Heald, S. M.; Villora, E. G.; Shimamura, K; Zheng, S.; Dunham, S. T.; Ohuchi, F. S.; Olmstead, M. A *J. Appl. Phys.* 2012, *111*, 123716.
(56) Sinha, G.; Adhikary, K.; Chaudhuri, S. *J. Cryst. Growth* 2005, *276*, 204.
(57) Zhou, X. T.; Heigl, F.; Ko, J. Y. P.; Murphy, M. W.; Zhou, J. G.; Regier, T.; Blyth, R. I. R.; Sham, T. K. *Phys. Rev. B* 2007, *75*, 125303.